Optical Materials 70 (2017) 165–170

Contents lists available at ScienceDirect

Optical Materials

journal homepage: www.elsevier.com/locate/optmat

Absorption enhancement in nanostructured silicon fabricated by self-assembled nanosphere lithography

Qiang Li [a, b], Jinsong Gao [a, b], Zizheng Li [a, *], Haigui Yang [a], Hai Liu [a], Xiaoyi Wang [a], Yudong Li [a]

[a] Key Laboratory of Optical System Advanced Manufacturing Technology, Changchun Institute of Optics, Fine Mechanics and Physics, Chinese Academy of Sciences, Changchun, 130033, China
[b] University of the Chinese Academy of Sciences, Beijing, 100039, China

ARTICLE INFO

Article history:
Received 2 May 2017
Received in revised form
18 May 2017
Accepted 19 May 2017
Available online 23 May 2017

Keywords:
Subwavelength structures
Nanostructures
Surface plasmons
Super absorber

ABSTRACT

In this work, we give a detailed experimental and theoretical analysis of a nano cone array on silicon wafer, which can greatly enhance the absorption compared with the polished silicon. The experimental absorptance can reach 98.7% in the wavelength ranging from 400 nm to 1100 nm. The mechanism of absorption enhancement is attributed to the nano cone array that can suppress the reflection by building a grade index from air to silicon surface. Moreover, an ultrathin 13 nm thickness gold film was sputtered on the nano cone array, by which surface plasmon can be excited and the absorption in the near-infrared region can be greatly enhanced. We also give a deep comprehending on the physics mechanism of such high absorption. This kind of nano cone array can be fabricated by a simple and low-cost colloidal sphere lithography and reactive ion etching, which makes it a more appropriate candidate for photovoltaics, spectroscopy, photodetectors, sensor, especially for the silicon-based application in the near-infrared region.

1. Introduction

It is well known that silicon (Si) is the most widely used for photodetectors [1] and solar cells [2–4] among semiconductor materials because it has many great advantages such as low cost, high performance and mature fabrication processes. Si as a kind of semiconductor material, is typically used to absorb photons and generate electron-hole pairs leading to the flow of photocurrent. However, flat silicon surface has high natural reflectance of around 30%–40% in the visible region, which degrades the efficiency of photoelectric conversion [5]. What is worse, to generate the electron-hole pairs inside a semiconductor, the energy carried by the incident electromagnetic wave should be higher than the bandgap of the semiconductor. So the large energy bandgap (1.12 ev) of Si decides silicon-based applications are mainly concentrated in the visible range (less than 1100 nm) [6]. Therefore, enhancing the absorption of Si become a topic of great interest especially in the near-infrared region, because it has the potential to extend silicon-based optoelectronic devices into the longer wavelength region (>1100 nm). Although many groups used femtosecond laser to fabricate black silicon that can also enhance the light trapping effect, increasing the optical absorption [7–9], this kind of textured surface structures produced by laser ablation are usually on micrometer scale, the size and aspect ratio of the surface structures are limited by the laser processing parameters.

In recent years, surface plasmon (SP) around metallic nanostructure provides an unprecedented way to rout and manipulate light on a nanoscale, which plays a vital role in various fields such as color filter [10–12], surface-enhanced Raman scattering (SERS) [13,14], extraordinary optical transmission (EOT) [15,16], sensor [17,18], and energy harvest [19–23]. SP is generated by coherent oscillations of free electrons coupled to an incident electromagnetic field, which is categorized into propagating surface plasmons (PSPs) and localized surface plasmons (LSPs). When the metal surface is in contact with a semiconductor forming a Schottky barrier, the SP excited by the nano metal structure can create energetic or hot electrons through nonradiative decay process, and these hot electrons can be injected into the conduction band of the neighboring semiconductor materials before thermalization resulting in photocurrent [24]. In this case, the barrier energy can

* Corresponding author.
E-mail address: lizizheng87@163.com (Z. Li).

http://dx.doi.org/10.1016/j.optmat.2017.05.036
0925-3467/

be much lower than the bandgap of the semiconductor, and the low-energy electrons can jump more easily into the conduction, which lays the fundamental of many silicon-based hot electron devices [25–28] in the near-infrared region. Moreover, the absorption peak can be tuned in a wide range by engineering the shape and size of the nano structure in order to achieve photoelectric response in the desired wavelength region. Many previous works have been widely studied both theoretically and experimentally in a variety of structures including metal grating [25], nanoparticles [26], nano cube [27], and nano hole [28]. However, these findings usually focus on a narrowed absorption band and the fabrication of these subwavelength nanostructures usually involves in electron beam lithography (EBL), which is costly and turns out to be a challenge for the application in large area. Despite these great achievements, it is still a challenge to realize efficient absorption in silicon-based devices with wide band especially in the near-infrared, and low cost, simple fabrication simultaneously.

In this paper, we used nanosphere lithography method to fabricate nano cone array on silicon (Si) wafer as Fig. 1 shows. This nano structure can reduce optical reflection of Si surface and enhance absorption efficiently in the visible spectrum. Moreover, an ultrathin 13 nm thickness gold (Au) film was sputtered on the nano cone array, by which surface plasmon can be excited and the absorption in the near-infrared region can be greatly enhanced. We also gave a comprehensive analysis on the enhancement mechanism by theory and experiment. The nano cone array on Si wafer is fabricated by a controlled colloidal sphere lithography, which has been widely exploited in the fabrication of nano structures, possessing advantages of large area, low cost, and easy fabrication process.

2. Experiment design and fabrication

We use a self-assembled nanosphere lithography to fabricate the nano cone array on the Si substrate, which is an efficient and inexpensive method to fabricate a large-area nanostructure. The procedure for the fabrication is shown in Fig. 1. Before making the PS sphere mask, silicon wafers (500 μm thickness, n-type (100)) were ultrasonically cleaned subsequently in acetone, ethanol, and distilled water for 30 min. The commercial PS spheres (700 nm) in an aqueous solution (10 wt %) were mixed up with equal volume of ethanol. Then the Si wafer were placed in a plastic box. The plastic box was filled up with deionized water. We use a syringe pump to inject the mixed PS sphere liquor onto the water surface at a rate of 3 μL/min. The PS spheres spread on the water surface and the surface tension forced the PS spheres to form a well-order monolayer over a large area on the water surface by the interface self-assembly method as the description in references [29,30]. The well-order monolayer would fall onto the surface of the Si wafer when the deionized water was drained out by a micropump. Then the Si wafer with the well-order PS sphere monolayer was kept in an annealing furnace at 180 °C for 5 min to make the PS spheres form good contact on the Si substrate. The size of the PS spheres was reduced by oxygen plasma using reactive ion etching (RIE) in a controlled manner. Afterward, we continued to etch silicon by RIE using SF_6 and O_2 plasma with 24 mTorr pressure, 50 w RF power, 48 sccm SF_6 flow rate, and 12 sccm O_2 flow rate. The formation mechanism of the nano cones can be understood by the chemical reactions during the RIE process. The active fluorine ions from the SF_6/O_2 plasma provide an etching effect to Si by forming the volatile SiF_4. As the etching rate of polystyrene sphere is much lower than that of Si under SF_6/O_2 plasma etching, polystyrene nanospheres protect Si immediately underneath them from being etched, resulting in the formation of nano cone array directly on Si wafer [31]. After RIE procedure, well-aligned nano cones can be formed on the entire silicon wafer. We removed the remaining PS nanospheres using ultrasonic cleaning in toluene solution for 10 min. Finally, an ultrathin 13 nm thickness Au film was coated on the silicon nano cones substrate by sputtering deposition in a vacuum chamber. In this fabrication process, the period can be adjusted by the different sizes of the PS spheres, the basal diameter and the height of the nano cone can be controlled by different etching time of the RIE procedure; the thickness of Au layer is determined by the deposition process. The experimental reflectance (R) and transmittance (T) are measured using a spectrometer (PerkinElmer Lambda-1050) equipped with a 160 mm integrating sphere. The experimental absorptance (A) is calculated by subtracting the sum of normalized reflectance and transmittance from unity.

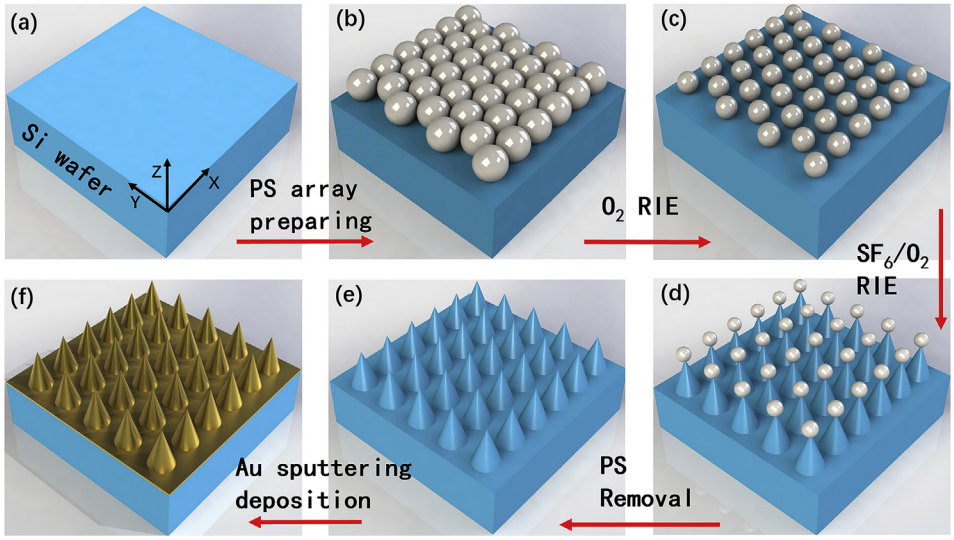

Fig. 1. Schematic illustration of the fabrication of nano cone array on silicon wafer. (a) A cleaned 500 μm thickness n-type Si (100) wafer. (b) A close packed PS monolayer template on the silicon wafer. (c) The size of the PS spheres was reduced by oxygen plasma etching. (d) Nano cone array with PS 'caps' was formed directly on Si wafer after SF_6/O_2 plasma etching. (e) The remaining PS nanospheres were removed. (f) Au film was coated on the nano cones by the method of RF reactive magnetron sputtering.

3. Experiment results and discussion

Fig. 2 shows the scanning electron microscopy (SEM) images of the PS monolayer and the nano structures fabricated by different etching durations. In Fig. 2(a), the PS nanospheres (700 nm) formed a close-packed monolayer on Si wafer in a hexagonal lattice, which displayed a high-quality order. Next, Fig. 2(b) shows that the size of the PS nanospheres was reduced after using an isotropic oxygen plasma etching for 10 s. This pattern served as an etch mask for the subsequent RIE processing of Si. Fig. 2(d)-(f) show three typical morphologies with an ultrathin 13 nm thickness Au coating, the morphologies formed after 70, 90 and 110 s SF_6/O_2 plasma etching respectively. Their basal diameter and height are indicated by the red arrows, which can be obtained by the cross-sectional views in Fig. 2(g)-(i). It should be pointed out that the 13 nm thickness Au film we sputtered on the nano structure formed a continuous thin film and did not turn into nano particles. Fig. 2(c) shows a fabricated sample with 13 nm Au film in large scale after 90 s SF_6/O_2 plasma etching.

Fig. 3 presents the experimental reflectance of polished Si wafer surface and the three different structural size of nano cones without Au film in the wavelength ranging from 400 to 2400 nm. The reflectance reduction achieved by the Si nano structure is very significant. For the polished Si wafer, most of the reflectance is greater than 35% in the visible region and about 55% in the near-infrared due to the large refractive index of Si, which leads to a high reflectance at the air–Si interface. In contrast, the antireflective nano cone array exhibits broad-band reflectance below 10% in the wavelengths from 400 nm to 1100 nm. Especially for the nano cone with H = 740 nm and P = 500 nm indicated by the red line in Fig. 2(h), the reflectance can reach as low as 1.3%, which is an amazing decrease compared with the polished Si wafer. However, in the longer wavelength region, the nano cone array may lose the ability of antireflection, and the reflectance still remains about 50% almost the same result as the polished Si.

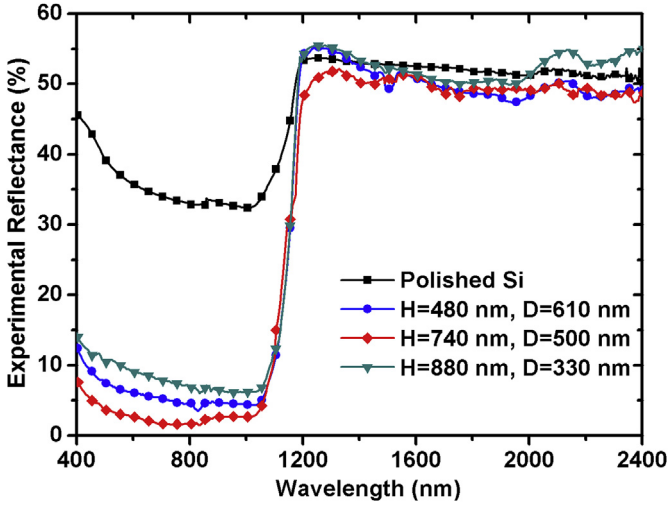

Fig. 3. The experimental measured reflectance of polished Si wafer and the three different structural sizes of nano cones in the wavelength ranging from 400 to 2400 nm.

The experimental absorptance (defined as A = 1-R-T) are shown in Fig. 4(a). As we can see, the absoptance in the wavelengths ranging from 400 to 1100 nm is ultra-high closely to 100%,

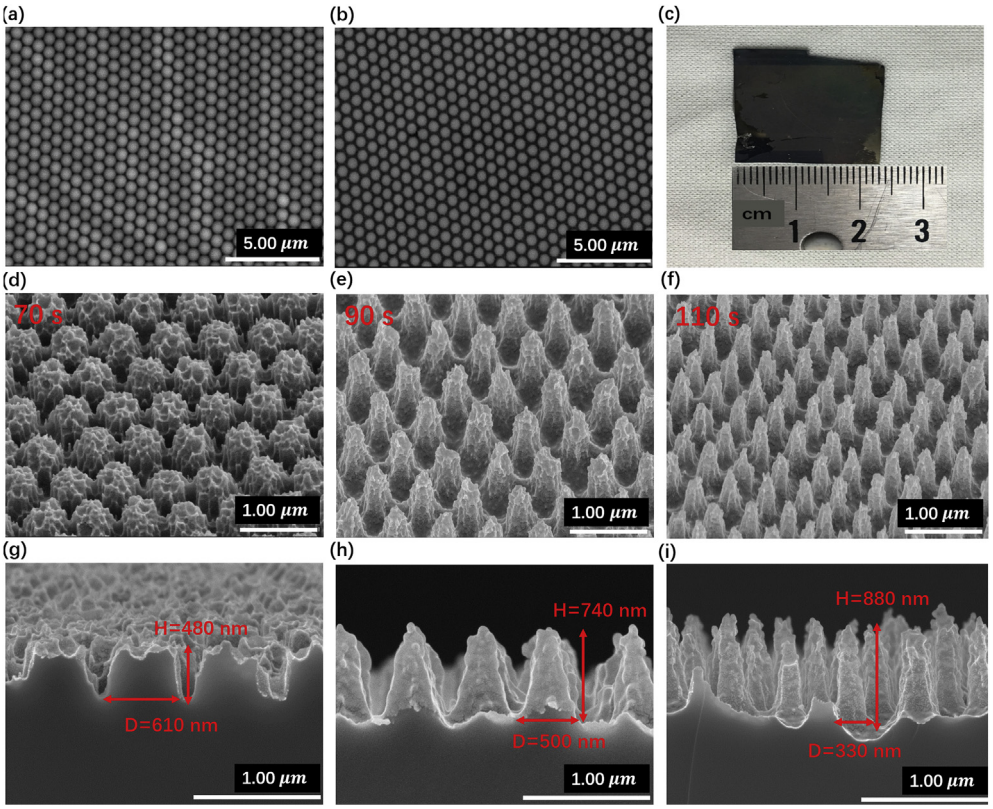

Fig. 2. SEM images of (a) Close packed PS monolayer template on the silicon wafer. (b) Non-closed packed PS spheres monolayer after oxygen plasma etching. (d), (e) and (f) Nano cone array after 70, 90 and 110 s SF_6/O_2 plasma etching respectively. All of them were coated by an ultrathin 13 nm thickness Au film. (g), (h) and (i) The cross-sectional views of the nano cone array taken from (d), (e) and (f) respectively. (c) Photo of a fabricated sample with 13 nm Au film in large scale after 90 s SF_6/O_2 plasma etching.

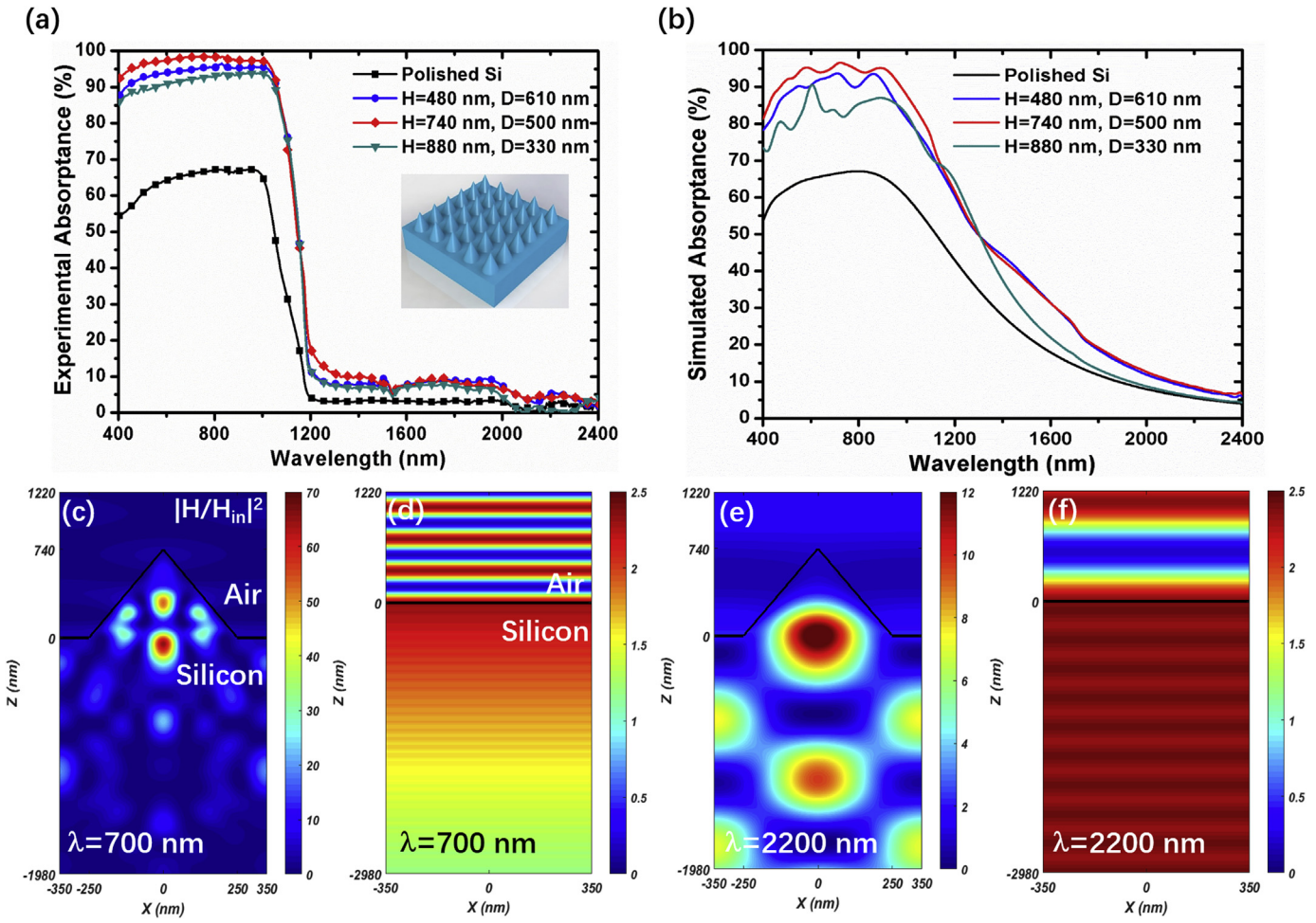

Fig. 4. (a) and (b) Experimental and simulated absorptance spectrums for polished and three nano structured silicon before Au film sputtering. (c)–(f) The FDTD simulation of the cross-sectional (in the x-z plane) relative magnetic field intensity distribution at the wavelengths of 700 nm and 2200 nm for nano cone array and silicon wafer, respectively. The period, height and basal diameter of the cone are 700 nm, 740 nm and 500 nm respectively.

suggesting that the absorption is almost completely. While the absoptance above the wavelength of 1200 nm is very low corresponding to little absorption. In order to verify the reflectance and absorptance spectrums obtained from the experiments, we perform the 3D finite-difference time-domain (FDTD) simulation to investigate the optical characteristic of the proposed nano cone array on Si substrate, where the periodic boundary conditions are used for a unit cell in the x-y plane and perfectly matched layers (PML) are applied along the z axis. The optical constants of Si used in the simulation are extracted from the data of Palik [32]. The incident light with a wavelength range from 400 nm to 2400 nm propagates along the negative z axis direction with the E field polarization in the x direction. The absorptance is calculated by the equation Absorptance = 1-Reflectance-Transmittance. The simulated absorptance spectrums are shown in Fig. 4(b), from which we can see that the simulated results fit the experiment results well. It should be noted that the experimental results still have some deviation from the simulation, which maybe originate from the fact that the shape of the nano cone fabricated by the self-assembled nanosphere lithography method is not a standard cone structure used in the simulation.

In addition, the FDTD simulation of the cross-sectional relative magnetic field intensity distribution at the wavelengths of 700 nm and 2200 nm with and without nano cone array were obtained as illustrated in Fig. 4(c)-(f) to further shed light on how the light couples into the nano cone. Compared with Figs. 3 and 4(c) and 4(d), we can safely come to the conclusion that for the short wavelength such as 700 nm, the absorption enhancement mainly results from the antireflection. The nano cone array suppresses the reflection by building a grade index from air to silicon surface. The grade index comes from the fact that the Si nano cone formed by RIE process provides an increasing radius cross section from the top to bottom of the cone which results in a height-dependent index as the reference describes [31]. This grade index, independent of wavelength, leads to couple a broadband incident light into the cone. As Fig. 4(c) illustrates the magnetic field is strongly localized inside the nano cone, which proves that the incident electromagnetic wave energy can be efficiently coupled into the nano cone and be consumed there due to the material property of the Si because the short wavelength electromagnetic wave cannot transmit too long in the silicon. Fig. 4(d) shows how the electromagnetic wave ($\lambda = 700$ nm) propagates when it impinges to the Si surface without nano cone array. The relative magnetic field decays obviously as the incident light penetrates into the Si wafer caused by the absorption of Si. While for the longer wavelength such as 2200 nm in Fig. 4(e) and (f), the intensity of the localized magnetic field in the nano cone is much weaker than it in Fig. 4(a), this is because the wavelength of the incident light is much larger than the size of the nano cone leading to the weaker ability of localizing incident light. Moreover, due to the material property of the Si, the transmission is

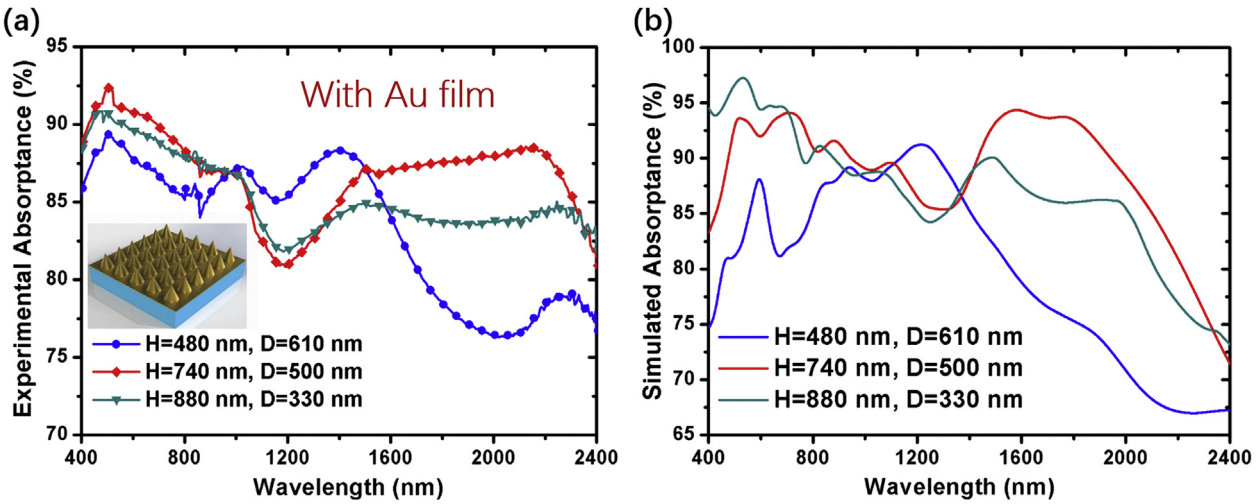

Fig. 5. (a) and (b) Experimental and simulated absorptance spectrums for three nano structured silicon after 13 nm Au film sputtering.

very high, which also a limiting for improving absorption in longer wavelength band.

In the previous section, we have demonstrated the nanocone array on the Si substrate can significantly reduce the reflection and enhance the absorption in the wavelength ranging from 400 nm to 1100 nm as well as its physical mechanism. However, the absorption from 1200 nm to 2400 nm presents almost the same result as the polished Si in Fig. 4(a), which limits the application of silicon-based device in the near-infrared region. Many previous works have demonstrated that metal nano structures on silicon substrate can enhance the absorption overcoming the constraints of the silicon bandgap by exciting surface plasmon [24–28]. On this basis, we further analyze the absorption enhancement in the wavelength ranging from 1200 nm to 2400 nm by sputtering an ultrathin (13 nm) Au film on the surface of nanocones. The experimental absorptance of three different structural sizes with Au film are shown in Fig. 5(a). The existence of the Au film can significantly suppress the reflection and transmission leading to a high absorption. As we can see, the absorption especially in near-infrared region ranging from 1200 nm to 2400 nm is greatly enhanced contrast with the absorption of nano cone array on the silicon wafer without Au film in Fig. 4(a), from which we can obtain that the ultra-thin Au film plays a vital role in the absorption enhancement mechanism. The simulated absorptance performed by FDTD algorithm is shown in Fig. 5(b), which fits the experimental results well. The optical constant of Au used in the simulation is extracted from the data of Johnson & Christy [33].

In order to clarify the physical mechanism of the absorption enhancement in the longer wavelength region after Au film sputtering, the FDTD simulation of the cross-sectional (in the x-z plane) relative magnetic field intensity distribution at the wavelengths of 1200 nm, 1500 nm, 1800 nm and 2200 nm were obtained as illustrated in Fig. 6(a)-(d). From Fig. 6, we can clearly see that the Au film on the nano cone can form a metal cavity which can greatly enhance the ability of localizing incident electromagnetic wave energy. And the intensity of magnetic field is much stronger contrast with Fig. 4(e) when the nano cone is not covered by Au film. Fig. 6(a) and (b) illustrate the magnetic field distribution at the wavelengths of 1200 nm and 1500 nm where the magnetic field is mainly localized in the Si cone, the nature of the localized surface plasmons. On the other hand, from Fig. 6(c) and (d) the magnetic field is mainly confined at the Si/Au interface, which indicates that the propagating surface plasmons mode is excited. The excitation of LSPs and PSPs makes a common contribution to the broadband and

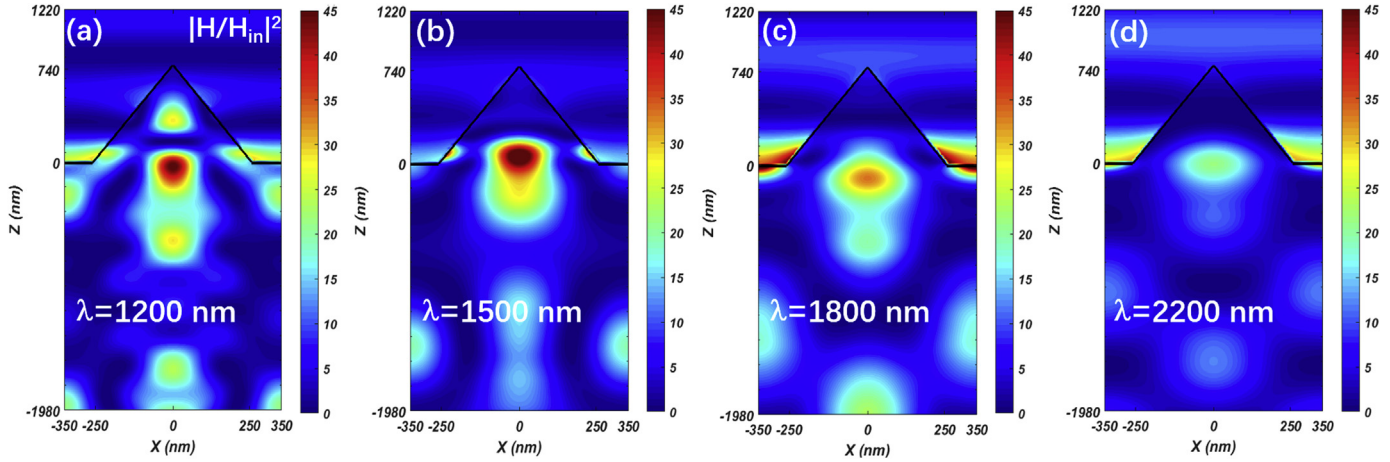

Fig. 6. (a)–(d) The relative magnetic field distribution at the wavelengths of 1200 nm, 1500 nm, 1800 nm and 2200 nm on the x-z plane for the nano cone with 13 nm Au film. The period, height and basal diameter of the cone are 700 nm, 740 nm and 500 nm respectively.

high absorption in the near-infrared wavelength because both of them can generate hot electrons when they decay through non-radiative process [24–28], which lays the fundamental of many silicon-based hot electron devices and provides a new perspective for the application of silicon-based device in the near-infrared region.

4. Conclusion

To summarize, we use a simple and low-cost colloidal sphere lithography and reactive ion etching to successfully fabricate a silicon-based super absorber in the visible and infrared spectrum. The ultrahigh absorptance can be achieved 98.7% in the visible region due to the fact that the Si nano cone can form a grade index from air to silicon surface leading to antireflection. Moreover, we further enhance the absorption in the wavelength from 1200 nm to 2400 nm by sputtering an ultrathin 13 nm Au film that can be used to extend Si photoelectric response into the near-infrared region. We thoroughly analyzed the physical mechanism of the absorption enhancement, which can be attributed to the excitation of LSPs and PSPs. This kind of silicon-based absorber provides a new perspective in photovoltaics, spectroscopy, photodetectors, sensor, especially for the silicon-based application in the near-infrared region.

Acknowledgments

Project supported by the National Natural Science Foundation of China (Nos. U1435210, 61306125, 61675199, and 11604329), the Science and Technology Innovation Project (Y3CX1SS143) of CIOMP, the Science and Technology Innovation Project of Jilin Province (Nos. Y3293UM130, 20130522147JH, and 20140101176JC).

References

[1] Z. Huang, J.E. Carey, M. Liu, X. Guo, E. Mazur, J.C. Campbell, Appl. Phys. Lett. 89 (2006) 033506.
[2] J. Oh, H.C. Yuan, H.M. Branz, Nat. Nanotechnol. 7 (2012) 743.
[3] C.M. Hsu, C. Battaglia, C. Pahud, Z. Ruan, F.J. Haug, S. Fan, C. Ballif, Y. Cui, Adv. Energy Mater 2 (2012) 628.
[4] J. Yang, F. Luo, T.S. Kao, X. Li, G.W. Ho, J. Teng, X. Luo, M. Hong, Light Sci. Appl. 3 (2014) e185.
[5] H.P. Wang, K.T. Tsai, K.Y. Lai, T.C. Wei, Y.L. Wang, J.H. He, Opt. Express 20 (2012) A94.
[6] J.E. Carey, C.H. Crouch, M. Shen, E. Mazur, Opt. Lett. 30 (2005) 1773.
[7] A.Y. Vorobyev, C. Guo, Appl. Surf. Sci. 257 (2011) 7291.
[8] Y. Ma, H. Ren, J. Si, X. Sun, H. Shi, T. Chen, F. Chen, X. Hou, Appl. Surf. Sci. 261 (2012) 722.
[9] G. Feng, Y. Wang, Y. Li, J. Zhu, L. Zhao, Mater. Lett. 65 (2011) 1238.
[10] Y.S. Do, K.C. Choi, Opt. Lett. 40 (2015) 3873.
[11] F. Cheng, X. Yang, D. Rosenmann, L. Stan, D. Czaplewski, J. Gao, Opt. Express 23 (2015) 25329.
[12] X.L. Hu, L.B. Sun, B. Zeng, L.S. Wang, Z.G. Yu, S.A. Bai, S.M. Yang, L.X. Zhao, Q. Li, M. Qiu, R.Z. Tai, H.J. Fecht, J.Z. Jiang, D.X. Zhang, Appl. Opt. 55 (2016) 148.
[13] Y. Chu, M.G. Banaee, K.B. Crozier, ACS Nano 4 (2010) 2804.
[14] A.G. Brolo, E. Arctander, R. Gordon, B. Leathem, K.L. Kavanagh, Nano Lett. 4 (2004) 2015.
[15] A. Peera, R. Biswas, Nanoscale 8 (2016) 4657.
[16] X. Zhou, S. Wen, B. Tang, D. Yang, J. He, Opt. Mater 52 (2016) 14.
[17] B. Park, S.H. Yun, C.Y. Cho, Y.C. Kim, J.C. Shin, H.G. Jeon, Y.H. Huh, I. Hwang, K.Y. Baik, Y.I. Lee, H.S. Uhm, G.S. Cho, E.H. Choi, Light Sci. Appl. 3 (2014) e222.
[18] T. Allsop, R. Arif, R. Neal, K. Kalli, V. Kundrat, A. Rozhin, P. Culverhouse, D.J. Webb, Light Sci. Appl. 5 (2016) e16036.
[19] Q. Li, Z. Li, H. Yang, H. Liu, X. Wang, J. Gao, J. Zhao, Opt. Express 24 (2016) 25885.
[20] M. Piralaeea, A. Asgari, Opt. Mater 62 (2016) 399.
[21] J. Wang, M. Zhu, J. Sun, K. Yi, J. Shao, Opt. Mater 62 (2016) 227.
[22] C.F. Guo, T.Y. Sun, F. Cao, Q. Liu, Z.F. Ren, Light Sci. Appl. 3 (2014) e161.
[23] Y. Li, B. An, S. Jiang, J. Gao, Y. Chen, S. Pan, Opt. Express 23 (2015) 17607.
[24] M.W. Knight, H. Sobhani, P. Nordlander, N.J. Halas, Science 332 (2011) 702.
[25] B.Y. Zheng, Y. Wang, P. Nordlander, N.J. Halas, Adv. Mater 26 (2014) 6318.
[26] Y.H. Su, Y.F. Ke, S. Cai, Q. Yao, Light Sci. Appl. 1 (2012) e14.
[27] W. Li, J. Valentine, Nano Lett. 14 (2014) 3510.
[28] K. Lin, H.L. Chen, Y.S. Lai, C.C. Yu, Nat. Commun. 5 (2014) 3288.
[29] J. Yu, Q. Yan, D. Shen, ACS Appl. Mater. Interfaces 2 (2010) 1922.
[30] P. Moitra, B.A. Slovick, W. Li, I.I. Kravchencko, D.P. Briggs, S. Krishnamurthy, J. Valentine, ACS Photonics 2 (2015) 692.
[31] K.Y. Lai, Y.R. Lin, H.P. Wanga, J.H. He, CrystEngComm 13 (2011) 1014.
[32] E.D. Palik, Handbook of Optical Constants of Solids, Academic, New York, 1998.
[33] P.B. Johnson, R.W. Christy, Phys. Rev. B 6 (1972) 4370.